MODELLING FUME DEPOSIT GROWTH IN RECOVERY BOILERS: EFFECT OF FLUE GAS AND DEPOSIT TEMPERATURE

AINO LEPPÄNEN*, HONGHI TRAN, ERKKI VÄLIMÄKI, ANTTI OKSANEN

ABSTRACT

The high ash content of black liquor causes fouling problems in the Kraft recovery boiler. The ash-forming elements condense into submicron-sized fume particles in the superheater area and the boiler bank and can deposit on heat-transfer surfaces. The fume deposits can then lower heat-transfer rate, plug flue gas flow, and expose surfaces to corrosion. This paper presents the results of a sensitivity analysis obtained using a CFD (computational fluid dynamics)-based sub-model of the formation of fume particles and deposits, showing how flue gas and deposit surface temperatures affect instantaneous fume deposit growth. The results indicate that fume deposit growth is a self-limiting process because the growth rate decreases as the deposit surface temperature increases. On the other hand, increasing the flue gas temperature increases the fume deposition rate when the element release factors are kept constant.

INTRODUCTION

Modern recovery boilers are designed to process high black liquor loads at high solids contents to produce steam efficiently. An inevitable side effect of this is increased temperatures in the lower furnace, which cause more ash-forming compounds to be released from the black liquor [1]. This in turn increases the propensity for fume formation and deposition on the tube surfaces in the superheater, boiler bank, and economizer regions of the boiler. The ash-forming elements, sodium (Na), potassium (K), chlorine (Cl), and sulphur (S), are released mainly in gaseous form from the burning black liquor droplets [2]. These elements form compounds that condense into fume particles in the upper furnace when the flue gas temperature decreases.

Fume particles form by condensation, which distinguishes them from larger carryover particles. Carryover particles originate mainly from entrainment of unburned black liquor droplets. Because of this difference, the deposition mechanisms of carryover particles, which are based on the fraction of melt in the particles [3], are not likely to be applicable to fume particles. Furthermore, because fume particles are small, < 1 µm, the fraction of melt in them does not likely play a role in fume deposition. The main cause of fume deposition is thermophoresis [4], which drives small fume particles from the hot flue gases toward the cooler tube surfaces. The significance of thermophoresis in the recovery boiler has been experimentally confirmed by Cameron and Georg-Wood [5].

Understanding the formation of fume particles and deposits is important. In modern boilers, improved boiler design and better operating strategies have significantly reduced the concentration of carryover particles in the flue gas. As a result, fumes form a larger part of deposits than in older boilers. However, similarly to carryover deposits, fume deposits also lower the heat transfer rate in the superheaters by acting as an insulating layer. They may even plug flue gas passages if the deposit layer is thick enough. This can be problematic, particularly in the boiler bank, where tube spacing is tight. Aged fume deposits are typically well sintered. They can be hard and tenacious on tubes and can become difficult to remove [1].

CFD (Computational Fluid Dynamics) modelling of recovery boilers was started in the 1980s and 1990s by Grace *et al.* [6] and Karvinen *et al.* [7]. In recent years, CFD modelling of recovery boilers has become more advanced and more detailed, particularly with respect to carryover deposits (e.g., Mueller *et al.* [8] and

AINO LEPPÄNEN
Tampere University of Technology, Finland

HONGHI TRAN
Pulp & Paper Centre
University of Toronto
Toronto ON, Canada

ERKKI VÄLIMÄKI
Valmet Power
Finland

ANTTI OKSANEN
Tampere University of Technology, Finland

*Contact: aino.leppanen@tut.fi

Li *et al.* [9]). However, modelling of fume formation in the recovery boiler has been attempted by only one research group in the 1990s [4,10,11]. This group developed a 1-D (one-dimensional) ABC model, which was later developed into a 2-D model [12], but its capabilities were limited by the low computational power available at that time. Verrill and Wessel [13] have also modelled alkali metal release and the subsequent fume yield, but not the actual fume formation process. To the authors' knowledge, no 3-D model for fume formation has been developed to date.

A CFD sub-model for alkali metals and fume particles has been developed and was presented in earlier publications by the authors [14,15]. The model has also been partially validated using actual measurements in a Finnish recovery boiler [16]. This paper discusses the results of a sensitivity analysis using the CFD sub-model. The analysis was conducted by changing two boundary conditions of the model: the deposit thickness on the primary superheater, and the flue gas temperature at the superheater entrance. It is important to test model sensitivity to such changes in boundary conditions so that the effects of such changes under real boiler conditions can be simulated.

MODELLING METHOD

The CFD sub-model was based on the ANSYS Fluent software [17], which was used to model gas flow, species transport, and black liquor combustion. The aim was to obtain realistic temperature and flow fields in the boiler, but not to focus on droplet behaviour, and therefore black liquor combustion was modelled using a simplified approach. The temperature field was considered accurate enough when the modelled temperature values fell within ± 60°C of the temperature measurements. Unlike the combustion reactions, reactions of ash-forming elements (Na, K, S, and Cl) were modelled in more detail. These elements form alkali metal compounds (Na_2SO_4, Na_2CO_3, NaCl, K_2SO_4, K_2CO_3, and KCl) through reactions which were modelled as equilibrium reactions with the help of the Equilib module of FactSage [18].

The simulations were conducted in two separate computational grids. Black liquor combustion and release of ash-forming compounds occurred in the furnace grid, whereas particle formation occurred in the superheater grid. The output values of the furnace grid were used as input values to the superheater grid, and the equilibrium reactions of alkali metal compounds were calculated for both grids. In this paper, only the results for the superheater grid are presented, the geometry of which is shown in Fig. 1.

As can be seen in Fig. 1, the whole

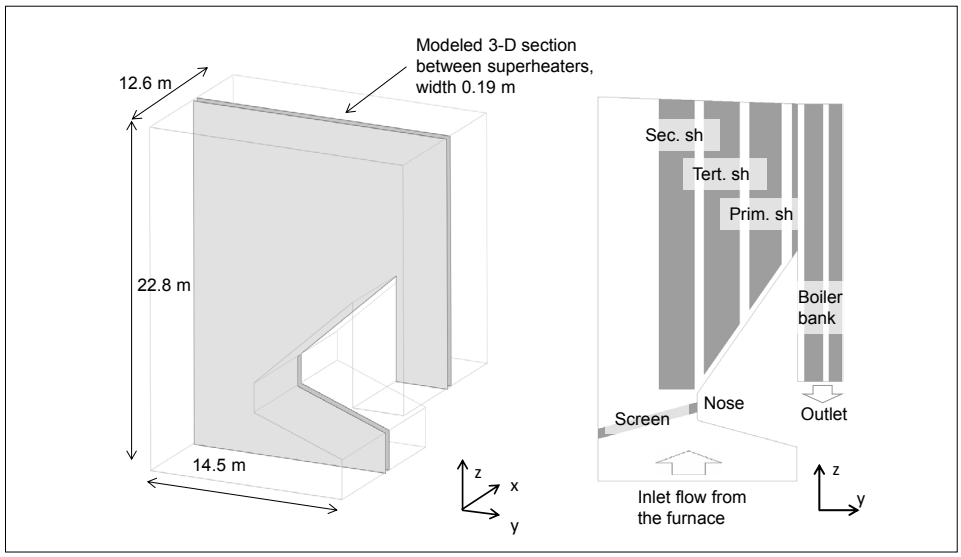

Fig. 1 - Schematic of the superheater area showing the modelled 3-D section between the superheaters (sh) and a 2-D projection of the modelled area with the names of the superheaters.

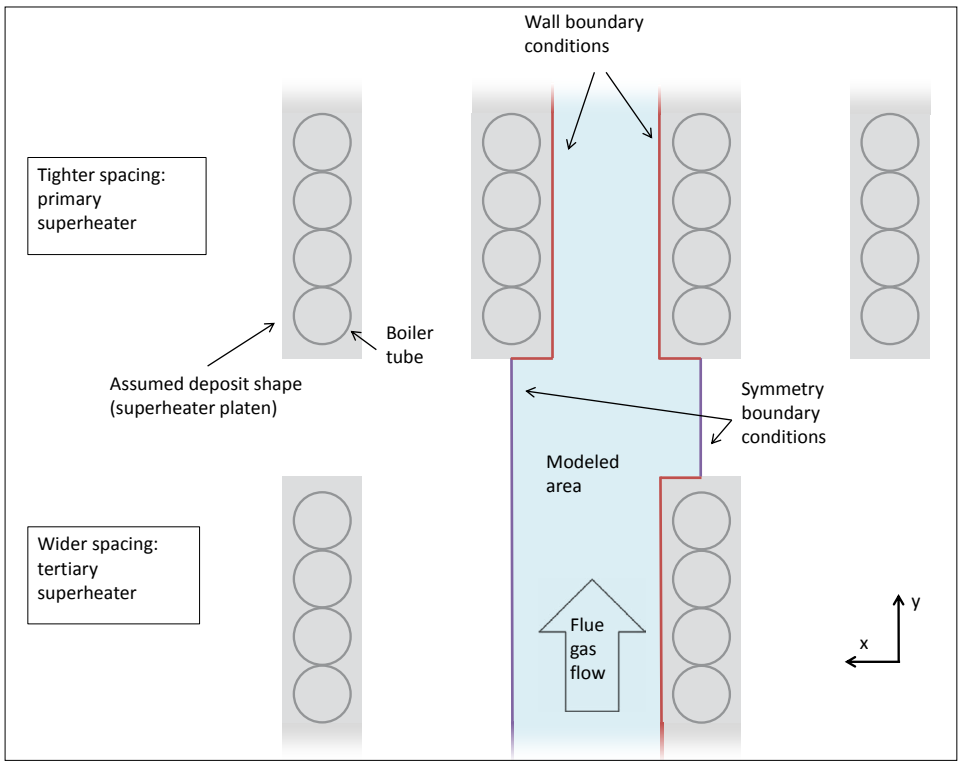

Fig. 2 - Schematic of the superheater platens between the tertiary and the primary superheater on the *y-x* plane.

superheater area was not simulated at once. Instead, a thin 3-D section in the middle of the superheater area was modelled. The sides of this section were modelled as symmetric boundary conditions or as walls in the vicinity of the superheater surfaces. A 2-D projection of the modelled area is also shown in Fig. 1 with the names of the various superheaters. The individual superheater tubes were not modelled, but the superheaters were treated as rectangular platens. This approach was taken because it was assumed that deposits had filled the cavities between individual tubes, as shown in Fig. 2. This figure illustrates how the superheater platens were modelled and which area was covered by the computational grid.

Figure 2 shows that the computational grid covered the area between the two superheater platens in areas of tighter tube spacing (the primary superheater and the boiler bank) and half the area between the two superheater platens in areas of wider tube spacing (the secondary and tertiary superheaters and the screen). The boundary conditions for the deposit surfaces and for the areas bounded by flue gas were the wall and the symmetric boundary condition respectively.

The computational grid of the superheater section in Fig. 1 was made up of 800,000 structured hexahedral cells. The flow and temperature fields were also calculated for grids with 1.4 and 2.4 million cells, but the results were not different from those for the 800,000-cell grid. Fume formation was also modelled using the 1.4 million-cell grid, but the results for fume particle composition did not change because fume formation is highly dependent on temperature. The 800,000-cell grid was therefore chosen for the sensitivity analysis because the larger grids are computationally more demanding.

Fume particle formation was simulated with the help of the FPM (Fine Particle Model) program [19], which incorporates certain aerosol dynamic processes into ANSYS Fluent. The FPM uses an Eulerian approach to model particles, which means that the evolution of particle size distributions was simulated. This approach enabled modelling of high particle concentrations, unlike Lagrangian particle tracking. The most important process affecting the particle size distribution was condensation of alkali vapours on particles. Particle nucleation was not modelled because it was assumed that tiny inert particle seeds (e.g., metal oxides) always exist in the boiler. The assumption of inert nuclei was also made by Jokiniemi *et al.* [11] and Eskola *et al.* [4].

In addition to fume formation, deposition of fume particles was modelled, but this was incorporated into the model through user-defined functions. The deposition processes considered include thermophoresis and deposition by diffusion, although the effect of diffusion was found to be negligible. Inertial impaction was not modelled because it is important only for larger particles [20].

Thermophoretic velocity was modelled by the following equation [21]:

$$V_t = \frac{-3\nu\nabla T_{gw}}{4\left(1+\frac{\pi\alpha}{8}\right)T_{ave}}, \quad (1)$$

where ν is the kinematic viscosity, ∇T_{gw} the temperature gradient between the flue gas and the wall, T_{ave} the average temperature between the flue gas and the wall, and α the accommodation coefficient, which is usually about 0.9 [22]. The above equation is valid when the particle diameter $d_p << l$, where l is the mean free path of the gas molecules, which is true in almost the entire modelled area.

In addition to fume particle deposition processes, direct vapour condensation was also modelled. In this work, the direct vapour condensation flux was based on the approach proposed by Jokiniemi *et al.* [23]:

$$I_v = \frac{\mathrm{Sh}(T_g)[D_v(T_g)D_v(T_w)]^{1/2}}{d_c R_g} \left(\frac{p_v(T_g)}{T_g} - \frac{p_{vs}(T_w)}{T_w}\right), \quad (2)$$

where $\mathrm{Sh}(T_g)=0.023 \cdot \mathrm{Re}^{0.8}\cdot\mathrm{Sc}(T_g)^{0.4}$, $\mathrm{Re}=Vd_c/\nu$, and $\mathrm{Sc}(T_g)=\nu/D_v(T_g)$. The symbols T_g and T_w are the temperatures of the flue gas and the wall, ρ_g is the gas density, V the gas velocity, d_c the characteristic diameter, and D_v the diffusion coefficient of vapour. The direct vapour condensation flux is dependent on $p_v(T_g)$, the actual vapour pressure of the condensing gas, and on $p_{vs}(T_w)$, the saturation vapour pressure of that gas at the wall temperature.

Modelling Assumptions

For this CFD sub-model to capture the relatively complex phenomenon of fume formation, several simplifying assumptions had to be made. The model was assumed to be time-independent to reduce computational cost. This meant that the model results, such as the fume deposit growth rate, were instantaneous results under the given boundary conditions. Moreover, the deposits did not grow thicker with time, nor did they become thinner or get removed by sootblowers.

Another simplification was the division of the superheater tubes into superheater groups, as shown in Fig. 1. Each group had a constant wall temperature and a constant initial deposit thickness as boundary conditions. The tube wall temperatures were based on actual boiler steam temperatures, which were assumed to remain constant despite small changes in boiler operation. The wall temperatures were the average temperatures of the tubes in each superheater group. The initial deposit thickness on each superheater was chosen so that the modelled flue gas temperatures would be close to the measured gas temperatures. The chosen deposit thickness was assumed to represent a stationary situation in which the deposition rate equalled the rate of particle reentrainment caused by sootblowing and other erosion mechanisms. The boundary conditions used in the baseline simulation are shown in Table 1.

Because choosing the initial thickness of the deposits introduces a source of uncertainty into the model, the model sensitivity to deposit thickness was investigated in this paper. The sensitivity analysis was conducted by changing the initial deposit thickness of one superheater group at a time. The change was executed by

TABLE 1 *Boundary conditions for the baseline simulation.*

Superheater	Screen	Secondary superheater	Tertiary superheater	Primary superheater	Boiler bank
Metal temperature (°C)	316	407	467	343	312
Initial deposit thickness (mm)	30	48	56	34	21

modifying the computational grid and by changing the thermal wall boundary condition in the CFD program. This changed the heat transfer rate and the flue gas and deposit surface temperatures, which affected condensation and deposition behaviour.

The release of ash-forming elements from black liquor depends on their content in the black liquor and their release factors. The release factors used in this work were obtained based on boiler measurements available in the literature [2,24]. The release factors used in the model are shown in Table 2. They were assumed to be independent of temperature, although it is known that release of Na, K, and Cl increases with temperature, whereas release of S decreases [25,26]. In this analysis, however, the effect of temperature changes on the deposition process is of interest, and therefore the release factors were kept constant.

TABLE 2 *Release factors used in the model.*

Element	Na	K	S	Cl
Release (%)	12	17	18	34

Sensitivity analysis was also conducted by changing the temperature of the flue gas entering the superheater area while maintaining the shape of the temperature distribution. However, because the release factors of the elements involved were held constant, a change in flue gas temperature affected only the condensation and deposition behaviours of the alkali compounds.

RESULTS AND DISCUSSION

The recovery boiler modelled in this work was a Finnish boiler with a capacity of 3400 t_{ds}/d. The boiler was running at almost full load. A comparison of the modelling results with the measurements was presented in a previous article by the authors [16]. At the time of the measurements, the boiler was burning black liquor with 79.3% dry solids content and the composition shown in Table 3.

Fume formation and deposition were first modelled for a baseline simulation in the superheater area of a recovery boiler. The results of the baseline simulation were presented in detail in the earlier article [16]. The modelling results showed that fume deposits grew fastest on the primary superheater. This result was also supported by the observation that the modelled boiler occasionally experienced massive deposit buildup at the same location.

According to the model, the main fume deposition mechanism is thermophoresis, which is dependent on the kinematic viscosity, the temperature gradient, and the average temperature between the flue gas and the deposit surface. On the other hand, these properties are dependent on certain boundary conditions of the model. To test model sensitivity to these parameters, a sensitivity analysis was conducted. In the first part of the sensitivity analysis, the thickness of the initial deposit on the primary superheater was changed, and in the second part, the flue gas temperature at the entrance of the superheater area was changed.

TABLE 3 *Composition of black liquor (dry mass basis).*

Element	C	H	S	O	N	Cl	Na	K	Inert
Wt%	33.5	3.4	6.5	34.5	0.1	0.06	20.8	0.9	0.2

Changing Initial Deposit Thickness on the Primary Superheater

The assumed initial deposit thickness on the primary superheater was an important boundary condition because it affected the instantaneous fume deposit growth rates calculated by the model. In the baseline case, the initial deposit thickness on the primary superheater was chosen to be 34 mm because this resulted in a flue gas temperature drop similar to that observed in the measurements. To determine the sensitivity of the modelling results, two other deposit thicknesses were used, as presented in Table 4.

The modelling results for instantaneous fume deposit growth rates for each superheater are shown in Fig. 3 for the baseline simulation (A) and the two new simulations (B and C). In Fig. 4, the same results are presented as average instantaneous growth rates over each superheater. The results for the various simulations are shown in reverse order (i.e., from lower to higher deposit thickness) to visualize how the deposit growth rate changes as the deposit grows. When calculating the growth rate, a deposit density of 1500 kg/m^3 was assumed. Fume deposits are porous when they form, but their density may increase because of sintering [1], and therefore deposit density can only be approximated.

In all these simulations, fume deposit growth seemed to be concentrated in the primary superheater, as can be seen in Fig. 3. This occurred because there the temperature difference between the flue gas and the deposit surface was significant and the superheater surfaces were closer to each other than in the earlier superheaters. Both these factors contributed to a high temperature gradient between the flue gas and the deposit surfaces, which increased deposition by thermophoresis (see Eq. 1). In addition, a small but significant fume deposition location was found where the flue gas flow turned downwards at the beginning of the boiler bank. Here, the thermophoretic velocity increased due to the high turbulent kinetic energy and high kinematic viscosity of the flue gas.

Figures 3 and 4 show that when the initial deposit thickness on the primary

TABLE 4 *Initial deposit thicknesses on the primary superheater in the various simulations.*

Case	A (baseline)	B	C
Deposit thickness (mm)	34	27	20

superheater was thinner (cases B and C), more fume particles deposited on the primary superheater. In all simulated cases, the flue gas temperatures were low enough for alkali sulphates and carbonates to condense onto particles already at the beginning of the superheater area, and therefore the location of particle growth did not cause this difference in the fume deposit growth rate. Instead, in cases B and C, more fume deposition occurred by thermophoresis because a thinner initial deposit decreased deposit thermal resistance, which cooled down the flue gas, especially near the deposit surface. This led to a larger temperature gradient and a smaller average temperature between the flue gas and the deposit surface, which both contributed to increased thermophoresis (see Eq. 1). This observation also means that, in general, the fume deposit growth rate slows down as the deposit thickness grows. This indicates that fume deposition, at least when dominated by thermophoresis, is a self-limiting process.

According to the modelling results, the deposit thickness seemed to move toward a steady-state condition. In reality, however, deposit growth is also limited by sootblowing, which was not modelled in this work. Furthermore, fume deposit growth completely stops if the deposit surface temperature reaches the radical deformation temperature, or T_{70} (the temperature at which the deposit contains 70 wt% molten phase) [3]. However, due to the low chlorine content of the black liquor, this temperature is unlikely to be reached in the primary superheater and boiler bank deposits.

When the initial deposit thickness on the primary superheater was reduced (cases B and C), there seemed to be less fume deposition in the boiler bank. This change seems to have been caused by the small decrease in kinematic viscosity of the flue gas, but the effect was not obvious. Another reason for the decreased fume deposition rate was that the fume particle concentration in the flue gases was lower because a significant proportion of the particles had already deposited on the primary superheater. On the other hand, when the initial deposit on the primary superheater was thicker (case A), fume deposition on the boiler bank was slightly higher. This indicates that fouling of one superheater may increase fume deposition on other surfaces downstream. This phenomenon has previously been observed for carryover deposition. Fouling in one location increases temperatures downstream, and the higher temperatures enable carryover particles to stick onto surfaces further into the superheater area [1].

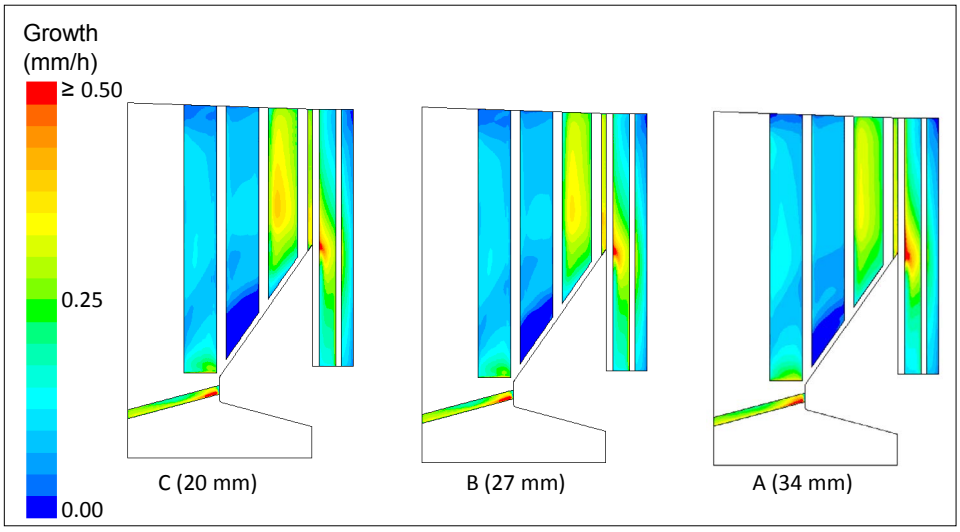

Fig. 3 - Instantaneous fume deposit growth rate (mm/h) on the various superheater surfaces with changes in the initial deposit thickness on the primary superheater.

Not all alkali compounds experience similar condensation and deposition behaviour. Alkali chlorides (NaCl and KCl) have significantly higher saturation vapour pressures than alkali sulphates and carbonates, and therefore they start to condense at lower temperatures. In the modelled boiler, alkali chloride condensation occurs at the flue gas temperatures prevailing at the primary superheater (about 800°C). Consequently, changes in flue gas and deposit temperatures can affect the chlorine content of the fume deposits in the primary superheater. Figure 5 shows the instantaneous chlorine content of the fumes depositing on the primary superheater in

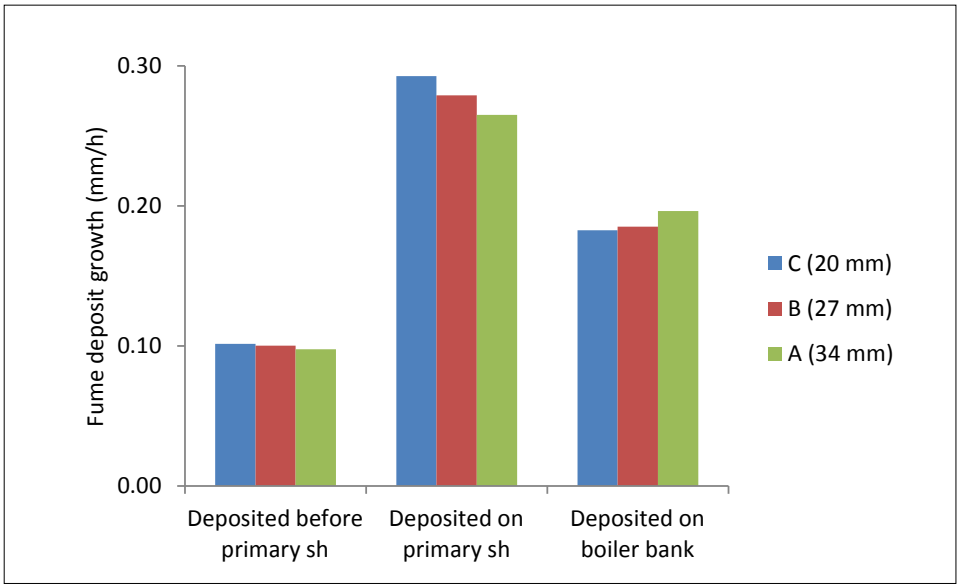

Fig. 4 - Average instantaneous fume deposit growth rates (mm/h) on the various superheater surfaces with changes in the initial deposit thickness on the primary superheater.

the various simulations. Except for chlorine content, fume deposit composition did not change among the various simulation cases. This was the case because only condensation of alkali chlorides occurred in the simulated temperature range.

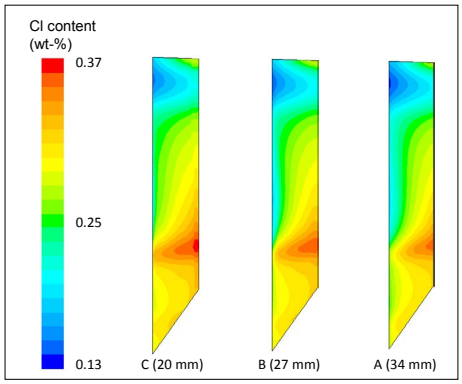

Fig. 5 - Average instantaneous Cl content (wt%) of fumes depositing on various superheater surfaces with changes in the initial deposit thickness on the primary superheater.

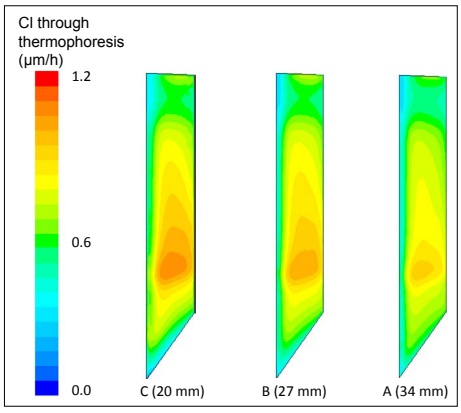

Fig. 6 - Instantaneous rate of chlorine deposition through thermophoresis (µm/h) on the primary superheater.

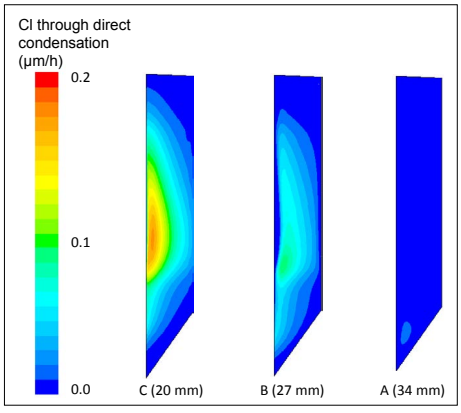

Fig. 7 - Instantaneous rate of direct condensation of chlorine (µm/h) on the primary superheater.

The modelling results showed a small decrease in deposit Cl content on the primary superheater when the deposit thickness increased. The reason for this can be understood when the contribution of the different deposit formation mechanisms is examined. Figure 6 shows the quantity of chlorides that deposit through thermophoretic movement of fume particles, and Fig. 7 shows the quantity of chlorides that condense directly from the gases to the deposit surfaces. In reality, the depositing and condensing compounds are alkali chlorides (NaCl and KCl), but the results are shown here for chloride ions (the assumed deposit density is still 1500 kg/m^3).

Figure 6 shows that the instantaneous rate of chlorine deposition through thermophoresis decreased somewhat when the initial deposit thickness on the primary superheater increased. This occurred because slightly higher flue gas temperatures allowed fewer alkali chlorides to condense onto fume particles because the alkali chlorides became supersaturated further downstream. On the other hand, a decreased temperature gradient and an increased average temperature between the flue gas and the deposit surface decreased particle deposition through thermophoresis, as previously explained.

The instantaneous rate of direct condensation of chlorine decreased significantly when the initial deposit thickness increased, as shown in Fig. 7. This occurred due to the higher deposit surface temperatures, which decreased the supersaturation of alkali chloride vapours near the deposit surface. However, the contribution of direct condensation of chlorine was still much smaller than the contribution of chlorine deposition through thermophoresis because most of the alkali chlorides condensed onto particles and not directly onto surfaces.

Figure 5 showed that the chlorine content of deposits can decrease when the initial deposit thickness increases. This indicates that in a situation where the deposit would be very thin, for example after sootblowing, the Cl content of the depositing fume layer could be significantly high. In addition, this high temperature dependence of alkali chloride condensation and deposition may be one of the reasons why more alkali chlorides are found in deposits closer to tube surfaces. Another potential explanation is that the alkali chlorides may vaporize in the hottest parts of the deposit, be transported towards the cooler temperatures, and condense near the tube surface [27]. However, it is possible that the deposits in recovery boilers are not porous enough to enable such transportation.

Changing Flue Gas Inlet Temperature

Another important boundary condition in the model is the temperature of the flue gas entering the superheater area. In the baseline case, the temperature distribution at the inlet is based on the simulation results in the furnace grid and on temperature measurements in the real boiler. Therefore, the inlet temperature, which varies between 930°C and 1080°C, is a more reliable boundary condition than the initial deposit thickness on the superheater. However, in real boiler operation, the flue gas temperature may change as a result of changes in liquor firing load or heating value, and therefore sensitivity analysis concerning the flue gas inlet temperature is relevant. Table 5 shows the results of various simulation cases where flue gas inlet temperature was varied.

TABLE 5 *Changes in flue gas inlet temperature in various simulations.*

Case	D	A (baseline)	E
Change in temperature (°C)	-50	0	+50

Figure 8 shows the results for average deposit growth rate on each superheater for the baseline simulation and the new simulations (D and E). The results are presented for a flue gas flow rate of 3.09 kg/s. The sensitivity analysis was performed by changing the temperature of the flue gas entering the superheater area while maintaining the shape of the temperature distribution.

Figure 8 shows that increasing the flue gas inlet temperature increases deposition on the superheater and the boiler bank surfaces. This occurs because the

temperature gradient between the flue gas and the deposit surfaces becomes larger, which increases deposition by thermophoresis. Note that in reality, the increase in fume deposition could be even greater, because at higher furnace temperature, more sodium is released from the black liquor [25]. However, the release factors were kept constant in these simulations. Furthermore, it seems that the chlorine content of the deposits decreases as the flue gas inlet temperature increases because alkali chlorides are less saturated at higher temperatures. However, the results for deposit chlorine content are not presented here because most likely the chlorine content is significantly dependent on the release factors.

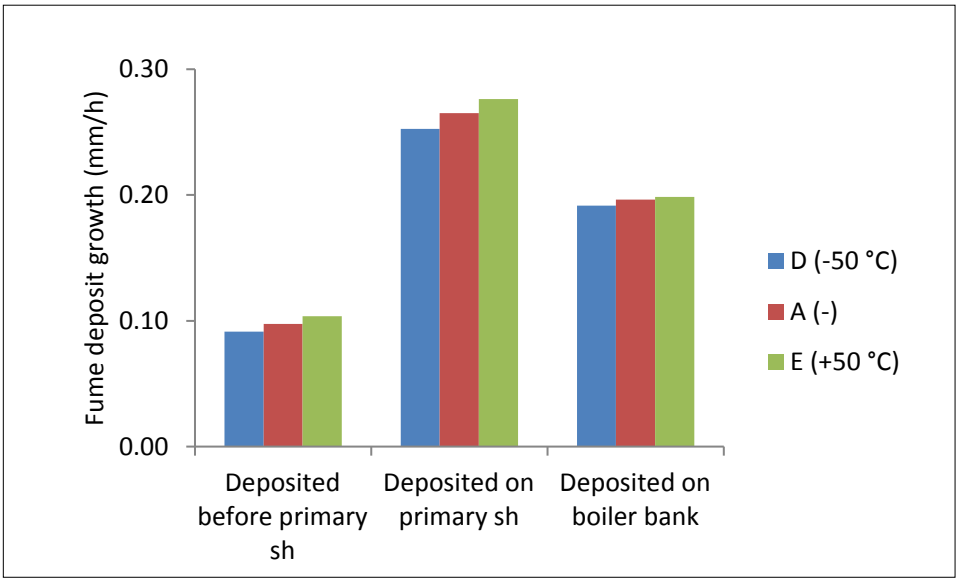

Fig. 8 - Average instantaneous fume deposit growth rates (mm/h) on various superheater surfaces with changes in flue gas inlet temperature. The results are presented for a flue gas flow rate of 3.09 kg/s.

CONCLUSIONS

A sensitivity analysis was performed using a CFD sub-model developed for fume formation and deposition. The aim was to examine the effects of initial deposit thickness and flue gas inlet temperature on fume formation and deposition in a recovery boiler. In all simulated cases, the primary superheater was the main fume deposition location because there the thermophoretic velocity was high due to the large temperature gradients between the flue gas and the deposit surfaces.

The results of the sensitivity analysis showed that when the deposit thickness on the primary superheater increases, the fume deposit growth rate on that superheater decreases. This occurs mostly because the temperature gradient between the flue gas and the deposit surface decreases, which lowers the rate of deposition by thermophoresis. Therefore, fume deposition seems to be a self-limiting process. Moreover, the thinner the deposit thickness is, the more alkali chlorides the deposit surface contains, because deposition and direct condensation of alkali chlorides are highly temperature-dependent processes.

The sensitivity analysis also indicated that the hotter the flue gas temperature, the more fume deposition occurs on the superheater and in the boiler bank area. This is again due to the increasing temperature gradient between the flue gas and the deposit surface, although the increase in the fume deposition rate is relatively small when the release factors of the elements are held constant.

ACKNOWLEDGEMENTS

The authors express their appreciation to Valmet Power and Tampere University of Technology for financing this project.

REFERENCES

1. Tran, H., "Upper Furnace Deposition and Plugging", in Adams, T. (ed.), Kraft Recovery Boilers, TAPPI Press, Atlanta, pp. 245-282 (1997).
2. Tamminen, T., Kiuru, J., Kiuru, R., Janka, K., and Hupa, M., "Dust and Flue Gas Chemistry during Rapid Changes in the Operation of Black Liquor Recovery Boilers: Part 1 - Dust Formation", TAPPI Journal, 1(5), pp. 27-32 (2002).
3. Tran, H., "How Does a Kraft Recovery Boiler Become Plugged", TAPPI Journal, 69(11), pp. 102-106 (1986).
4. Eskola, A., Jokiniemi, J., Lehtinen, K., and Vakkilainen, E., "Modelling Alkali Salt Deposition on Kraft Recovery Boiler Heat Exchangers in the Superheater Section", Proceedings of the 1998 International Chemical Recovery Conference, p. 469 (1998).
5. Cameron, J.H. and Georg-Wood, K., "Role of Thermophoresis in the Deposition of Fume Particles Resulting from the Combustion of High Inorganic Containing Fuels with Reference to Kraft Black Liquor", Fuel Processing Technology, 60(1), pp. 49-68 (1999).
6. Grace, T., Walsh, A., Jones, A., Sumnicht, D., and Farrington, T., "A Three-Dimensional Mathematical Model of the Kraft Recovery Furnace", Proceedings, 1989 International Chemical Recovery Conference (1989).
7. Karvinen, R., Hyöty, P., and Siiskonen, P., "The Effect of Dry Solids Content on Recovery Boiler Furnace Behaviour", TAPPI Journal, 74(12), pp. 171-177 (1991).
8. Mueller, C., Selenius, M., Theis, M., Skrifvars, B., Backman, R., Hupa, M., and Tran, H., "Deposition Behaviour of Molten Alkali-Rich Fly Ashes—Development of a Submodel for CFD Applications", Proceedings of the Combustion Institute, 30(2), pp. 2991-2998 (2005).
9. Li, B., Brink, A., and Hupa, M., "CFD Investigation of Slagging on a

Super-Heater Tube in a Kraft Recovery Boiler", Fuel Processing Technology, 105, pp. 149-153 (2013).
10. Jokiniemi, J., Lazaridis, M., Lehtinen, K., and Kauppinen, E., "Numerical Simulation of Vapour-Aerosol Dynamics in Combustion Processes", Journal of Aerosol Science, 25(3), pp. 429-446 (1994).
11. Jokiniemi, J., Pyykönen, J., Mikkanen, P., and Kauppinen, E., "Modeling Fume Formation and Deposition in Kraft Recovery Boilers", TAPPI Journal, 79(7), pp. 171-181 (1996).
12. Pyykönen, J. and Jokiniemi, J., "Modelling Alkali Chloride Superheater Deposition and its Implications", Fuel Processing Technology, 80(3), pp. 225-262 (2003).
13. Verrill, C.L. and Wessel, R.A., "Detailed Black Liquor Drop Combustion Model for Predicting Fumes in Kraft Recovery Boilers", TAPPI Journal, 81(9), pp. 139-148 (1998).
14. Leppänen, A., Välimäki, E., and Oksanen, A., "Modeling Fine Particles and Alkali Metal Compound Behaviour in a Kraft Recovery Boiler", TAPPI Journal, 11(7), pp. 9-14 (2012).
15. Leppänen, A., Välimäki, E., Oksanen, A., and Tran, H., "CFD: Modeling of Fume Formation in Kraft Recovery Boilers", TAPPI Journal, 12(3), pp. 25-32 (2013).
16. Leppänen, A., Tran, H.N., Taipale, R., Välimäki, E., and Oksanen, A., "Numerical Modeling of Fine Particle and Deposit Formation in a Recovery Boiler", Fuel, 129, pp. 45-53 (2014).
17. ANSYS Inc., ANSYS Academic Research, Release 14.0 (2011).
18. Thermfact & GTT Technologies, FactSage (The Equilib Module—Regular Features) (2009).
19. Particle Dynamics GmbH, Fine Particle Model (FPM) for FLUENT: User's Guide (2003).
20. Friedlander, S. Smoke, Dust, and Haze: Fundamentals of Aerosol Dynamics, Oxford University Press, New York (2000).
21. Waldmann, L., Schmitt, K., "Thermophoresis and Diffusiophoresis of Aerosols", in Davies, C. N., (ed.), Aerosol Science, Academic Press, London, pp. 137-162 (1966).
22. Whitby, E. and McMurry, P., "Modal Aerosol Dynamics Modeling", Aerosol Science and Technology, 27, pp. 673-688 (1997).
23. Jokiniemi, J., Pyykönen, J., Lyyränen, J., Mikkanen, P., and Kauppinen, E., "Modelling Ash Deposition during the Combustion of Low-Grade Fuels", in Baxter, L. and DeSollar, R. (eds.), Applications of Advanced Technology to Ash-Related Problems in Boilers, Plenum Press, New York, pp. 591-615 (1996).
24. Mikkanen, P., Fly Ash Particle Formation in Kraft Recovery Boilers, Dissertation, Helsinki University of Technology (2000).
25. Hupa, M., "Recovery Boiler Chemistry", in Adams, T. (ed.), Kraft Recovery Boilers, TAPPI Press, Atlanta, pp. 39-57 (1997).
26. Wåg, K.J., Reis, V.V., Frederick, W.J., and Grace, T.M., "Mathematical Model for the Release of Inorganic Emissions during Black Liquor Char Combustion", TAPPI Journal, 80(5), pp. 135-145 (1997).
27. Lindberg, D., Engblom, M., Yrjas, P., Laurén, T., Lindholm, J., and Hupa, M., "Influence of Deposit Aging on Superheater Corrosion", Proceedings of the 2014 International Chemical Recovery Conference, Volume 2, p. 101 (2014).